

**Tomographic
algorithms for Polar
Mesospheric Cloud
observations**

K. Hultgren et al.

Application of tomographic algorithms to Polar Mesospheric Cloud observations by Odin/OSIRIS

K. Hultgren¹, J. Gumbel¹, D. A. Degenstein², A. E. Bourassa², and N. D. Lloyd²

¹Department of Meteorology, Stockholm University, Stockholm, Sweden

²Department of Physics and Engineering Physics, University of Saskatchewan, Saskatoon, Canada

Received: 23 April 2012 – Accepted: 7 May 2012 – Published: 25 May 2012

Correspondence to: K. Hultgren (kristofferh@misu.su.se)

Published by Copernicus Publications on behalf of the European Geosciences Union.

[Title Page](#)

[Abstract](#)

[Introduction](#)

[Conclusions](#)

[References](#)

[Tables](#)

[Figures](#)

[⏪](#)

[⏩](#)

[◀](#)

[▶](#)

[Back](#)

[Close](#)

[Full Screen / Esc](#)

[Printer-friendly Version](#)

[Interactive Discussion](#)

Abstract

Limb-scanning satellites can provide global information about the vertical structure of Polar Mesospheric Clouds. However, information about horizontal structures usually remains limited. This is due to both a long line of sight and a long scan duration. On 5 eighteen days during the Northern Hemisphere summers 2010–2011 and the Southern Hemisphere summer 2011/2012, the Swedish-led Odin satellite was operated in a special mesospheric mode with short limb scans limited to the altitude range of Polar Mesospheric Clouds. For Odin's Optical Spectrograph and InfraRed Imager System (OSIRIS) this provides multiple views through a given cloud volume and, thus, a basis 10 for tomographic analysis of the vertical/horizontal cloud structure. Here we present algorithms for tomographic analysis of mesospheric clouds based on maximum probability techniques. We also present results of simulating OSIRIS tomography and retrieved cloud structures from the special tomographic periods.

1 Introduction

15 Downward imaging can provide detailed information about the horizontal structure of Polar Mesospheric Clouds (PMCs)¹ (McClintock et al., 2009). However, vertical information cannot be derived from nadir pointing instruments. Limb-scanning satellites are on the other hand able to provide global information about the vertical structure of PMCs but give a very diffuse horizontal picture due to a long line of sight and long scan duration. When investigating atmospheric phenomena like PMCs, it is essential 20 to obtain local structures to understand the global picture. To retrieve two-dimensional vertical/horizontal information, a technique that can handle both vertical and horizontal inhomogeneity is needed. Tomographic methods applied to limb-scanning measurements are such techniques.

¹Also denoted as Noctilucent Clouds (NLC) when viewed from the ground.

Tomographic algorithms for Polar Mesospheric Cloud observations

K. Hultgren et al.

Title Page

Abstract

Introduction

Conclusions

References

Tables

Figures

⏪

⏩

◀

▶

Back

Close

Full Screen / Esc

Printer-friendly Version

Interactive Discussion



Tomographic algorithms for Polar Mesospheric Cloud observations

K. Hultgren et al.

Title Page

Abstract

Introduction

Conclusions

References

Tables

Figures



Back

Close

Full Screen / Esc

Printer-friendly Version

Interactive Discussion



Forward directed satellite-based limb observations of PMC scattering from consecutive positions along the satellite orbit provide input to tomographic techniques. These techniques invert the observed brightness into an estimate of the volume emission rate and hence provide information about both the vertical and horizontal dimensions in a measurement plane that coincides with the satellite orbit plane. The quality of the resulting reconstruction is strongly dependent on the number of measurements along different lines of sight through the analyzed volume.

The ideal application of tomography is within the medical field where the term usually refers to Magnetic Resonance Imaging (MRI) or X-ray Computed Tomography (CT). In both cases, an imaging device is rotated around a patient, collecting data from every angle. In contrast, discrete limb observations from a moving spacecraft cover only a limited angular range. The method used in the current work is similar to the maximum likelihood expectation maximization technique, developed originally to recover two-dimensional positron emission fields in medical imaging of the human brain (Shepp and Vardi, 1982).

The history of tomography related to satellite measurements is limited and has so far focused on airglow emissions. The use of satellite limb measurements of tropical nightglow in the F region initiated the use of tomographic techniques in atmospheric sciences (Thomas and Donahue, 1972). Since then, various methods have been developed. The possibility of recovering airglow structures from limb emission profiles was first demonstrated by using an iterative maximum probability method by McDade and Llewellyn (1993). In the current work, we use an atmospheric model together with a tomographic algorithm that assumes no a priori information to examine the effectiveness of satellite limb tomography. The technique is applied to PMC radiance measured by the OSIRIS instrument onboard the Odin satellite, where each measurement is an integral of the volume emission taken along a line of sight. This is fundamental input to a tomographic technique that involves the discretization of the integrals and the allocation of volume emission rates to points in a discrete two-dimensional grid that is representative of the atmosphere.

Tomographic algorithms for Polar Mesospheric Cloud observations

K. Hultgren et al.

Title Page

Abstract

Introduction

Conclusions

References

Tables

Figures

⏪

⏩

◀

▶

Back

Close

Full Screen / Esc

Printer-friendly Version

Interactive Discussion



Compared to a limb-imaging technique where several lines of sight are collected simultaneously, OSIRIS is a limb-scanning instrument. This means that OSIRIS is only able to capture one line of sight per read-out, leading to a very coarse temporal resolution of the measurements. We show that the tomographic technique allows for the recovery of PMC structures despite the sparse data sampling.

This paper is divided into three main parts: first, we discuss the tomographic technique and a model for the atmosphere to which the algorithm is applied. Secondly, we present model simulations of OSIRIS measurements to test the possibilities of tomographic recoveries and to optimize settings applied to special tomographic modes uploaded to OSIRIS. Then, thirdly, we present data collected during these measurement modes and retrieve results from running the OSIRIS observations through the tomographic algorithm. We conclude with a discussion and an outlook on ongoing comparisons with other satellite instruments.

2 The tomographic technique

2.1 Atmospheric model

From the knowledge of a set of line integrals through a field $f(x,y)$ it is possible to reduce a tomographic problem to the solution of this field by inversion. The lines in Fig. 1 make up a set of discrete paths through a given point along which line integrals can be calculated. If it is possible to determine line integrals at every point within the field, and the angles between successive lines are infinitesimal, then these integrals can be reduced to the Radon transform (Herman, 1980). The inverse transform is then the solution for this field.

Observations from a satellite platform, however, have certain limitations compared to the method shown in Fig. 1. The solid Earth limits the look directions so that, for the atmosphere, only a very limited interval of viewing angles can provide line integrals through a given point. Figure 2 shows this scenario. The paths shown are tangent to the

Tomographic algorithms for Polar Mesospheric Cloud observations

K. Hultgren et al.

Title Page

Abstract

Introduction

Conclusions

References

Tables

Figures

⏪

⏩

◀

▶

Back

Close

Full Screen / Esc

Printer-friendly Version

Interactive Discussion



solid Earth and therefore represent limiting paths. For an observational point at 85 km, these limiting paths are separated by an angle $\theta \approx 20^\circ$. The possible lines of sight intersecting the given point are then all paths between these boundaries. The same angle θ is also, in a geocentric system, determining the movement of the satellite between positions 1 and 2 and thereby defines the “angle along the orbit” used throughout this paper. For a satellite speed of $\sim 7 \text{ km s}^{-1}$, this implies that the time interval between a set of boundary paths for a given point in the mesopause region is about 5 min. This time interval is consequently also the temporal scale for sampling a specific volume in space at 85 km.

As can be seen in Fig. 3, the atmosphere can be divided into a discrete emission grid. The grid cells are defined by the angle along the orbit and the radial distance from the centre of the Earth. They are labeled with an index j , increasing with atmospheric layer and angular division. The type of grid shown in Fig. 3 is used for three purposes in the tomographic algorithms; first, a grid is used to contain an atmospheric volume emission rate profile for the simulated observations – the emission grid. Secondly, a grid is used to store OSIRIS observations – the observation grid. Thirdly, a grid is used to store the retrieved profile from the tomographic inversions – the retrieval grid. These three grids, however, do not have the same resolution since the atmospheric volume emission rate in general needs a finer structure than is possible to obtain for the resulting retrievals. Also, the retrieval grid must be optimized with respect to the satellite geometry and the power of the available computing equipment to provide an accurate and efficient solution. The size parameters used are discussed further below.

2.2 Tomographic algorithm

The mathematical basis for tomographic imaging was laid down by Johann Radon during the beginning of the 20th century when he published the basis for the “Radon transform” (Radon, 1917). This paper tells us that if we have an infinite number of one-dimensional projections of an object taken at an infinite number of angles, we can perfectly reconstruct the original object by finding the inverse Radon transform. The

2004), solves the problem in an iterative fashion where the iteration is performed on a ray by ray basis until the algorithm converges. The expression is given by

$$V_j^{(k)} = V_j^{(k-1)} \sum_i \left(\frac{O_i}{O_{i_{\text{est}}^{(k-1)}}} \beta_{ij} \right) \quad (3)$$

where the superscripts (k) and ($k - 1$) indicate the current and previous iterations, respectively.

$$O_{i_{\text{est}}}^{(k-1)} = \sum_j L_{ij} V_j^{(k-1)}$$

represents an estimated observation of a single line of sight based on the forward model outlined above together with the previous estimate of the volume emission and

$$\beta_{ij} = \frac{L_{ij}}{\sum_i L_{ij}}$$

is an observation weighting filter acting as an averaging kernel which determines the relative effect of each observation on the convergence of the tomographic inversion.

The algorithm starts with an initial estimate of the source distribution $V_j^{(1)}$. The choice is of primary importance for the applicability of the method and for the number of iterations. In our case, the observations provide an initial value that starts the iterative process. The initial estimate is given by the MART technique as

$$V_j^{(1)} = \sum_i \left(\frac{O_i}{\sum_i L_{ij}} \beta_{ij} \right) \quad (4)$$

and is thus the weighted average over all observations using the assumption that the profile is uniform along each line of sight.

Tomographic algorithms for Polar Mesospheric Cloud observations

K. Hultgren et al.

Title Page

Abstract

Introduction

Conclusions

References

Tables

Figures

◀

▶

◀

▶

Back

Close

Full Screen / Esc

Printer-friendly Version

Interactive Discussion



2.3 Overall retrieval scheme

Figure 4 shows a block diagram of the tomographic process. The primary inputs are the radiance measurements (the observations) made by OSIRIS. Also required as input is a set of ancillary data containing various satellite parameters, such as position and orientation of the spacecraft as well as the grid parameters defining minimum and maximum radial shell distances and radial and angular grid cell sizes. Figure 4 also shows (in red or grey, depending on online or printed reading) how the iterative process is implemented to produce the final volume emission. For the first iteration, the “compare” step is skipped and Eq. (4) is used as a first estimate for the volume emissions from each cell. For the next iteration the first estimate is used as input to estimated observations which are, in turn, compared with the actual observations and the process is repeated until the output converges, usually around 30 iterations. The focus of the present work is on the practical evaluation of the technique described above as used with the OSIRIS observations.

3 Simulation results used to configure Odin and OSIRIS for the tomographic mode

The OSIRIS measurements are, as already mentioned, integrations along lines of sight. This means that the measurements are functions of the optical path through the atmosphere. For test purposes and optimization of the tomographic algorithm, it is necessary to apply a forward model that describes the observations and to simulate the retrieval.

The first step of the modeling process is the creation of an arbitrary emission grid, $100\text{ m} \times 0.1^\circ$, as shown in Fig. 3. The measured brightness, defined by Eq. (2), is then simulated by using various vertical scan speeds as well as orbital and attitude parameters of Odin. These simulations are performed for successive lines of sight that represent the measured set provided by the satellite limb scans. This data is then

Tomographic algorithms for Polar Mesospheric Cloud observations

K. Hultgren et al.

Title Page

Abstract

Introduction

Conclusions

References

Tables

Figures



Back

Close

Full Screen / Esc

Printer-friendly Version

Interactive Discussion



interpolated to an observation grid, $125\text{ m} \times 0.1^\circ$ and, finally, the tomographic inversion is performed onto the observation grid creating a retrieval grid, $500\text{ m} \times 0.5^\circ$, which then is containing the recovered cloud structure. The grid cell sizes have been optimized based on the observation geometry.

5 Important parameters characterizing the simulations are the vertical scan speed and the read-out frequency of the limb spectra. Since there is a limit on the exposure times when observing the limb from a satellite platform, the read-out frequency cannot be made shorter than two seconds for OSIRIS. The vertical scan speed is more flexible. To be able to draw conclusions about which scan speed to use, the simulated observations
10 served as input to the tomographic retrieval algorithm. In this way, the parameters could easily be changed and finally tweaked to match the best recovery of the input volume emission profile. As a result, the best retrievals in terms of combined horizontal and vertical resolution were obtained for a scan speed of 0.5 km s^{-1} .

The result of a retrieval simulation is presented in Fig. 5. The top panel shows an
15 arbitrarily created input emission, a “test PMC”, on which the measurements were simulated. The second panel shows the same input emission but with the resolution reduced to the same as the tomographic retrieval grid. The third panel shows the simulated OSIRIS measurements, and the bottom panel shows the retrieved emission, i.e. the result of the tomographic algorithm using the simulated measurements as input. In the ideal case, the second and the bottom panels should thus be identical. We
20 see that this is not entirely true. However, the structures of the input and the output are, as shown below, very similar and thus considered satisfactory for the purpose of this work. Important to note here is that the second panel is only included as a comparison to the result – the data in the top panel is what is being sampled by the forward model.

25 Figure 6 shows the integrated vertical (black lines) and horizontal (grey lines) cross sections of the simulation results, corresponding to the second and the bottom panels of Fig. 5. It is apparent that the vertically integrated emissions, i.e. the measurements of a horizontal plane, are very well captured. However, the horizontally integrated emissions, measurements of a vertical plane, are slightly misplaced in altitude. Since the

Tomographic algorithms for Polar Mesospheric Cloud observations

K. Hultgren et al.

Title Page

Abstract

Introduction

Conclusions

References

Tables

Figures



Back

Close

Full Screen / Esc

Printer-friendly Version

Interactive Discussion



vertical resolution of OSIRIS observations is about 1 km, this offset of ~ 250 m still resembles the input emissions very well. It is also noticeable that the peak altitude of the cloud is reproduced.

The input emission includes a wave structure with wavelength $\sim 3.5^\circ$ (~ 380 km), also resolved in the recovered emission. This shows that waves of these scales should be able to be retrieved with the tomographic algorithm. On the contrary, smaller horizontal scales are unlikely to be captured. The possible vertical scales are limited by the scan speed and the retrieval grid cell size, which both are set to 0.5 km for this work and are thus resolved at ~ 1 km.

Simulations including noise have also been performed. The result showed that the tomographic algorithm is capable of successfully reproduce input emissions with induced noise levels of up to 4%. Noise levels larger than this limit will however have a large uncertainty on the output.

4 Odin and OSIRIS

The Odin satellite was launched on 20 February 2001 from Svobodny in Eastern Siberia. The satellite was placed into an almost circular Sun-synchronous orbit near 600 km with the ascending node at 18:00 local time and with a period of approximately 96 min (Murtagh et al., 2002; Llewellyn et al., 2004). Onboard Odin, two instruments are installed: the Sub-Millimeter Radiometer (SMR) and the Optical Spectrograph and InfraRed Imager System (OSIRIS). The Odin mission was designed as a shared mission for both astronomers and atmospheric scientists by looking out into deep space when performing astronomy measurements and down to Earth for atmospheric observations. For the latter purpose, the satellite is pointed towards the limb of the Earth, usually in the direction of the satellite track. When performing these limb measurements the entire satellite is nodded so that the co-aligned optical axes of SMR and OSIRIS sweep over selected altitude ranges.

Tomographic algorithms for Polar Mesospheric Cloud observations

K. Hultgren et al.

Title Page

Abstract

Introduction

Conclusions

References

Tables

Figures

⏪

⏩

◀

▶

Back

Close

Full Screen / Esc

Printer-friendly Version

Interactive Discussion



Tomographic algorithms for Polar Mesospheric Cloud observations

K. Hultgren et al.

Title Page

Abstract

Introduction

Conclusions

References

Tables

Figures

⏪

⏩

◀

▶

Back

Close

Full Screen / Esc

Printer-friendly Version

Interactive Discussion



OSIRIS is designed to retrieve altitude profiles of atmospheric minor species by observing limb-radiance profiles. The optical spectrograph obtains spectra of scattered sunlight over the range 275–810 nm with a spectral resolution of approximately 1 nm. For the analysis of PMCs, mainly ultraviolet wavelengths below 310 nm are used as absorption by stratospheric ozone at these wavelengths prevents complications due to upwelling radiation. Below 310 nm several wavelength intervals can be chosen that are free from perturbing airglow and auroral emissions (Karlsson and Gumbel, 2005). In the current work we have averaged over the wavelength interval 302.8–305.9 nm.

In order to extract PMC properties, the pure cloud radiance needs to be separated from the background radiation due to molecular Rayleigh scattering and instrumental effects. Instrumental effects result, e.g. from sensitivity of the instrument optics to radiation from below the nominal field-of-view in terms of baffle scattering (Llewellyn et al., 2004). Odin’s ordinary PMC analysis uses limb scans ranging from the troposphere to the lower thermosphere. This provides limb radiance profiles covering extensive height ranges below and above the PMC layer. Molecular and instrumental background can then readily be discriminated by fitting the data in these cloud-free altitude ranges (Karlsson and Gumbel, 2005). This procedure is not possible in the case of the concentrated tomography scans applied in the present work. As the tomographic scans are restricted to the narrow altitude region of the PMC, background fits to cloud-free altitude ranges above and below the PMC are not available. Instead, the molecular scattering background is calculated in terms of the altitude-dependent Rayleigh scattering by an atmospheric density profile from the MSIS climatology. The instrumental background is taken as the mean value of the background obtained from ordinary limb scans during the days before and after the tomography scans. These backgrounds are then subtracted from the measured total limb radiance in order to obtain the pure PMC signal as input to the tomographic retrieval. This use of “climatological” molecular and instrumental background introduces uncertainties as it ignores the scan-to-scan variability of these parameters. Based on ordinary non-tomographic PMC measurements,

these uncertainties in the PMC limb data can be estimated to be less than 1 % of the peak OSIRIS PMC radiances shown in Sect. 5.

There are two primary scan modes for the atmospheric mission: the stratospheric mode where the lines of sight cover altitudes between 7–67 km of the atmosphere and the stratospheric/mesospheric mode where the altitudes 7–107 km are covered. Odin usually operates in one of these two modes, but during the northern summers of 2010–2011 and the southern summer of 2011/2012 a special “tomographic mode” was incorporated for the orbit numbers shown in Table 1. This mode was based on the simulations presented above and concentrated on the altitudes 73 to 88 km for the first period (2010) and 77 to 88 km for the rest of the orbits. By performing these short scans, the horizontal distance between subsequent scans was significantly reduced. This strongly increased the number of lines of sight through a given volume and, consequently, allowed for a tomographic analysis using the technique outlined above to make a two-dimensional retrieval of the volume emission rate profile as a function of radial distance from the centre of the Earth and angle along the satellite track.

The tomographic mode was uploaded to Odin/OSIRIS to be used during a total of 270 orbits (these orbits were chosen as to provide coincident measurements with AIM/CIPS, further discussed below). In this way, Odin could focus more intensely on the PMC altitudes and maximize the number of lines of sight through the cloud.

5 Data and retrieval

Figure 7 shows an example of an OSIRIS observation set together with the corresponding tomographic recovery. The data in the top panel was used together with the technique discussed above to make a two-dimensional tomographic retrieval of the volume emission as a function of altitude and angle along the satellite track, shown in the middle panel of Fig. 7, where each angle corresponds to a unique latitude and longitude pair. The result has been interpolated to a resolution of $100\text{m} \times 0.01^\circ$. A dotted

Tomographic algorithms for Polar Mesospheric Cloud observations

K. Hultgren et al.

Title Page

Abstract

Introduction

Conclusions

References

Tables

Figures



Back

Close

Full Screen / Esc

Printer-friendly Version

Interactive Discussion



saw-tooth shaped pattern is showing the tangent positions of the original measurements.

A comparison of the two top panels shows that the clouds have been localized in the retrievals. As compared to the original limb data, the retrieved PMC structures are similar but noticeably different. Also, the relative magnitudes of the retrieved features are different from the features seen in the measurements. (A complete collection of the plots from the orbits listed in Table 1 can be found on <http://people.su.se/~krhu6073/tomoOS/>.)

To check the consistency of the algorithm, the recovered emissions have also been used as a base to predict OSIRIS measurements. In other words, the tomographic recoveries of OSIRIS observations are used as the emissions contained in the emission grid. Simulated measurements are then performed using these recoveries, yielding predictions of the observations. These predictions are exemplified in the bottom panel of Fig. 7 and it can be seen that the predictions agree well with the real observations and hence that the algorithm is consistent.

As noted earlier, the temporal scale for sampling a specific cloud volume at 85 km is about 5 min. PMCs are affected by gravity waves with periods less than 5 min (Witt, 1961), but at the horizontal scales resolved by the algorithm this time scale is considered not to provide any complications.

6 Discussion and conclusions

With this work we have demonstrated the possibility to perform tomographic investigations of middle atmospheric phenomena using the OSIRIS instrument on the Odin satellite. The motivation for this work has been to conduct the first tomographic analysis of PMCs. Therefore the settings of the algorithm presented here are specific for the Odin platform and the OSIRIS instrument. However, the Odin mission is not optimized for tomographic applications. A future instrument dedicated to tomography would need an imaging device that could sample brightness along different lines of sight

Tomographic algorithms for Polar Mesospheric Cloud observations

K. Hultgren et al.

Title Page

Abstract

Introduction

Conclusions

References

Tables

Figures



Back

Close

Full Screen / Esc

Printer-friendly Version

Interactive Discussion



Tomographic algorithms for Polar Mesospheric Cloud observations

K. Hultgren et al.

[Title Page](#)

[Abstract](#)

[Introduction](#)

[Conclusions](#)

[References](#)

[Tables](#)

[Figures](#)



[Back](#)

[Close](#)

[Full Screen / Esc](#)

[Printer-friendly Version](#)

[Interactive Discussion](#)



simultaneously. This would provide the possibility to sample the region of interest at a higher speed and thus obtain a much better horizontal resolution. If a new mission, focusing on tomographic methods, is to be planned, the ideal scenario would be to use a two-dimensional imager to produce three-dimensional retrievals. Including the nadir view would also enhance the measurements. However, one would then also need to accommodate for the albedo effects.

As noted earlier, only OSIRIS UV data around 304.3 nm are analyzed in this paper. By utilizing a broader wavelength range, spectral analysis can reveal information about PMC particle sizes. Ongoing work thus concerns the possibility to extend the tomographic analysis to the spatial distribution of particle sizes by using data from several wavelength intervals in the ultraviolet.

Work is currently also conducted to compare the retrieved PMC structures to images collected by the CIPS instrument aboard the AIM satellite. CIPS is a nadir pointing imager providing 900 km wide orbit strips that contains albedo of PMCs with a resolution of 25 m². Odin is placed in an orbit perpendicular to the AIM strips. In addition, the two satellites have very similar orbital periods, hence providing coincident measurements in common volume during overlapping parts of about 30 sequential orbits per 30 days. The coincident measurements during the total of the 270 events provided by the tomographic modes in the northern hemispheric summers of 2010 and 2011, discussed above, are currently being compared and used in a co-analysis of the two instruments. The tomographic retrievals are providing good sources for vertical information to complement the very detailed horizontal structures provided by CIPS.

The altitude region under examination in this paper is also the transition region between the middle and upper atmosphere. The state and variability of this region is controlled by wave dynamics from below, while waves acting upward cause variability in the thermosphere and ionosphere. The PMC region is therefore an important source of information for research that aims at merging the middle and upper atmosphere. In order to address the entire wave spectrum of this region, tomography in combination with limb imaging would be essential. In this scenario, the algorithm presented in this

paper would be able to reproduce wave signatures of down to ~ 100 km horizontally and 1 km vertically. Using a two dimensional imager would also provide a base for a future three dimensional tomographic retrieval.

Acknowledgements. We would like to thank SSC for making tomographic scans with Odin/OSIRIS possible. OSIRIS is funded in part by the Canadian Space Agency. We also thank the Climate Research School (CRS) within the Bert Bolin Centre for partially funding the project.

References

- Degenstein, D. A.: Atmospheric volume emission tomography from a satellite platform, PhD thesis, University of Saskatchewan, Saskatoon, 1999.
- Degenstein, D. A., Llewellyn, E. J., and Lloyd, N. D.: Volume emission rate tomography from a satellite platform, *Appl. Opt.*, 42, 1441–1450, 2003.
- Degenstein, D. A., Llewellyn, E. J., and Lloyd, N. D.: Tomographic retrieval of the oxygen infrared atmospheric band with the OSIRIS infrared imager, *Can. J. Phys.*, 82, 501–515, 2004.
- Frey, S., Mende, S. B., and Frey, H. U.: Satellite limb tomography applied to airglow of the 630 nm emission, *J. Geophys. Res.*, 106, 21367–21380, 2001.
- Herman, G. T.: *Fundamentals of Computerized Tomography: Image Reconstruction From Projections*, 2nd Edn., Academic Press, New York, 2009.
- Karlsson, B. and Gumbel, J.: Challenges in the limb retrieval of noctilucent cloud properties from Odin/OSIRIS, *Adv. Space Res.*, 36, 935–942, 2005.
- Llewellyn, E. J., Lloyd, N. D., Degenstein, D. A., Gattinger, R. L., Petelina, S. V., Bourassa, A. E., Wiensz, J. T., Ivanov, E. V., McDade, I. C., Solheim, B. H., McConnell, J. C., Haley, C. S., von Savigny, C., Sioris, C. E., McLinden, C. A., Griffioen, E., Kaminski, J., Evans, W. F. J., Puckrin, E., Strong, K., Wehrle, V., Hum, R. H., Kendall, D. J. W., Matsushita, J., Murtagh, D. P., Brohede, S., Stegman, J., Witt, G., Barnes, G., Payne, W. F., Piché, L., Smith, K., Warshaw, G., Deslauniers, D.-L., Marchand, P., Richardson, E. H., King, R. A., Wevers, I., McCreath, W., Kyrölä, E., Oikarinen, L., Leppelmeier, G. W., Auvinen, H., Mégie, G., Hauchecorne, A., Lefèvre, F., de La Nöe, J., Ricaud, P., Frisk, U., Sjöberg, F., von Schéele, F., and Nordh, L.: The OSIRIS instrument on the Odin spacecraft, *Can. J. Phys.*, 82, 411–422, 2004.

Tomographic algorithms for Polar Mesospheric Cloud observations

K. Hultgren et al.

Title Page

Abstract

Introduction

Conclusions

References

Tables

Figures

◀

▶

◀

▶

Back

Close

Full Screen / Esc

Printer-friendly Version

Interactive Discussion



Tomographic algorithms for Polar Mesospheric Cloud observations

K. Hultgren et al.

Title Page

Abstract

Introduction

Conclusions

References

Tables

Figures

⏪

⏩

◀

▶

Back

Close

Full Screen / Esc

Printer-friendly Version

Interactive Discussion



Lloyd, N. and Llewellyn, E. J.: Deconvolution of blurred images using photon counting statistics and maximum probability, *Can. J. Phys.*, 67, 89–94, 1989.

McClintock, W. E., Rusch, D. W., Thomas, G. E., Merkel, A. W., Lankton, M. R., Drake, V. A., Bailey, S. M., and Russell III, J. M.: The cloud imaging and particle size experiment on the aeronomy of ice in the mesosphere mission: instrument concept, design, calibration, and on-orbit performance, *J. Atmos. Sol.-Terr. Phys.*, 71, 340–355, doi:10.1016/j.jastp.2008.10.011, 2009.

McDade, I. C. and Llewellyn, E. J.: Satellite airglow limb tomography: methods for recovering structured emission rates in the mesospheric airglow layer, *Can. J. Phys.*, 71, 552–563, 1993.

Murtagh, D., Frisk, U., Merino, F., Ridal, M., Jonsson, A., Stegman, J., Witt, G., Eriksson, P., Jiménez, C., Megie, G., de la Noë, J., Ricaud, P., Baron, P., Pardo, J. R., Hauchcorne, A., Llewellyn, E. J., Degenstein, D. A., Gattinger, R. L., Lloyd, N. D., Evans, W. F. J., McDade, I. C., Haley, C. S., Sioris, C., von Savigny, C., Solheim, B. H., McConnell, J. C., Strong, K., Richardson, E. H., Leppelmeier, G. W., Kyrölä, E., Auvinen, H., and Oikarinen, L.: Review: an overview of the Odin atmospheric mission, *Can. J. Phys.*, 80, 309, doi:10.1139/p01-157, 2002.

Radon, J. and Parks, P. C. (Translator): On the determination of functions from their integral values along certain manifolds, *IEEE T. Med. Imaging*, 5, 170–176, doi:10.1109/TMI.1986.4307775, 1986.

Shepp, L. A. and Vardi, Y.: Maximum likelihood reconstruction for positron emission tomography, *IEEE T. Med. Imaging*, 1, 113–122, 1982.

Thomas, R. J. and Donahue, T. M.: Analysis of Ogo 6 observations of the OI 5577 – a tropical nightglow, *J. Geophys. Res.*, 77, 3557–3565, 1972.

Witt, G.: Height, structure and displacements of noctilucent clouds, *Tellus*, 14, 1–18, 1962.

Tomographic algorithms for Polar Mesospheric Cloud observations

K. Hultgren et al.

Table 1. Orbit numbers and days covered by the tomographic mode of Odin.

Days	Orbit numbers
15–17 Jun 2010	50775–50804
14–16 Jul 2010	51209–51238
12–14 Aug 2010	51642–51671
15–17 Jun 2011	56233–56261
17–19 Jul 2011	56711–56740
18–20 Aug 2011	57190–57219
29–30 Nov 2011	58729–58757
7–9 Jan 2012	59313–59343
14–16 Feb 2012	59911–59925

Title Page

Abstract

Introduction

Conclusions

References

Tables

Figures

⏪

⏩

◀

▶

Back

Close

Full Screen / Esc

Printer-friendly Version

Interactive Discussion



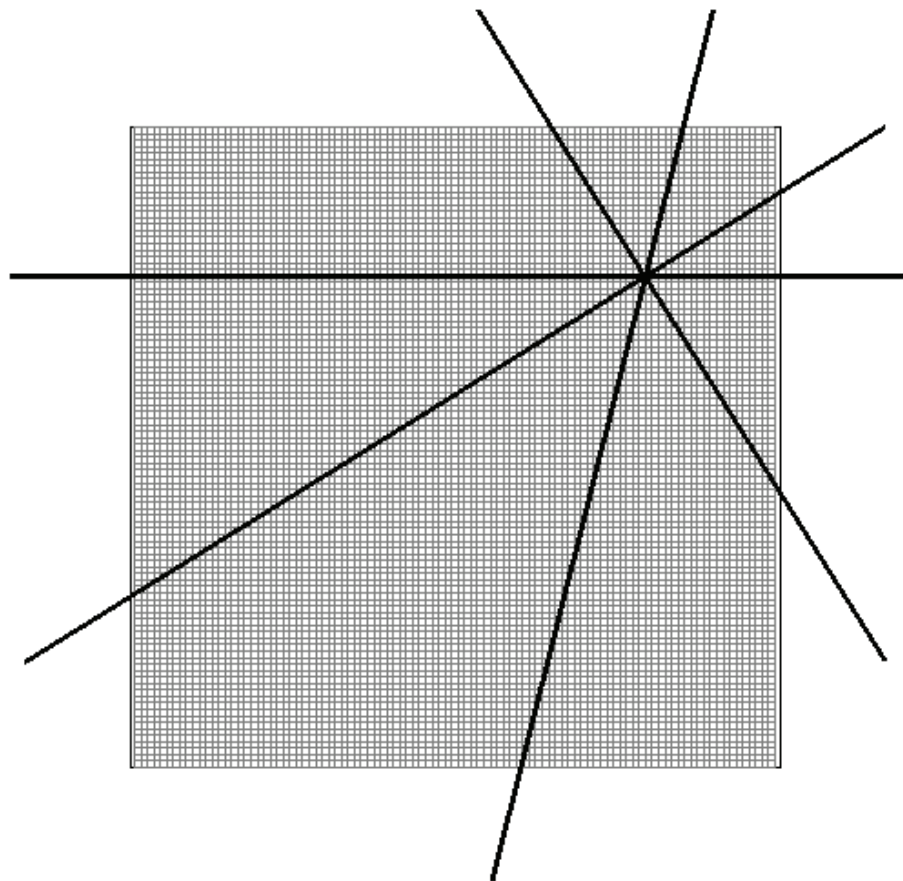


Fig. 1. A set of discrete paths through a given point in a field $f(x, y)$ along which line integrals can be calculated. If the angles between successive lines of this type are infinitesimal, the field can be solved for by the inverse Radon transform.

Tomographic algorithms for Polar Mesospheric Cloud observations

K. Hultgren et al.

Title Page

Abstract

Introduction

Conclusions

References

Tables

Figures

◀

▶

◀

▶

Back

Close

Full Screen / Esc

Printer-friendly Version

Interactive Discussion

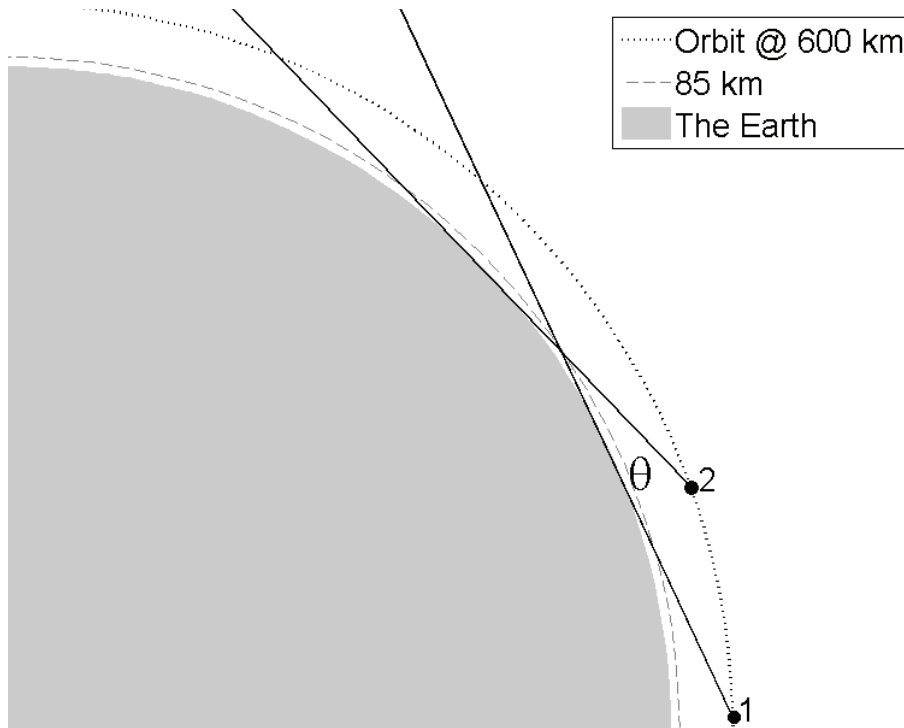


Fig. 2. The viewing interval for tangent lines through a point at 85 km over which line integrals can be calculated. The points 1 and 2 represent the limiting satellite positions from where this point can be seen (to scale).

Tomographic algorithms for Polar Mesospheric Cloud observations

K. Hultgren et al.

Title Page	
Abstract	Introduction
Conclusions	References
Tables	Figures
◀	▶
◀	▶
Back	Close
Full Screen / Esc	
Printer-friendly Version	
Interactive Discussion	



Tomographic algorithms for Polar Mesospheric Cloud observations

K. Hultgren et al.

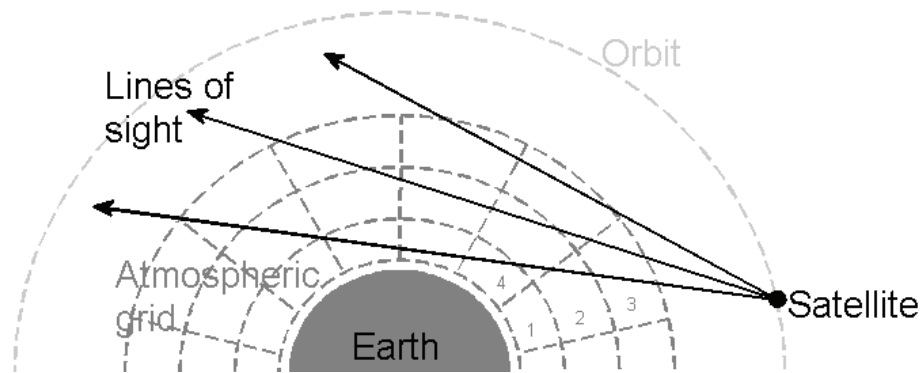


Fig. 3. A two-dimensional emission grid used for multiple purposes, explained in the text (not to scale).

Title Page	
Abstract	Introduction
Conclusions	References
Tables	Figures
⏪	⏩
◀	▶
Back	Close
Full Screen / Esc	
Printer-friendly Version	
Interactive Discussion	



Tomographic algorithms for Polar Mesospheric Cloud observations

K. Hultgren et al.

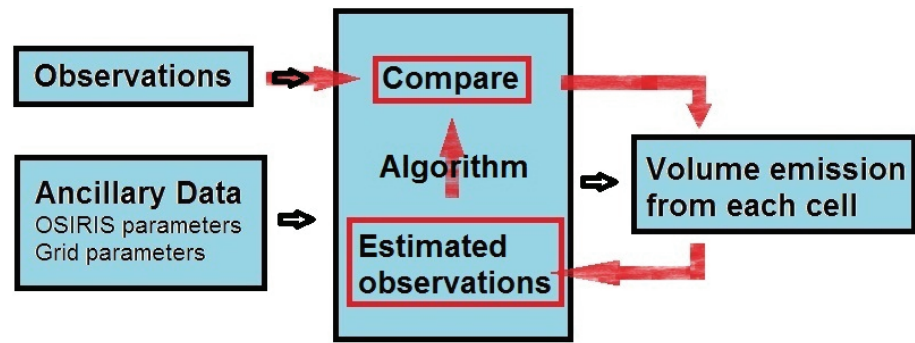


Fig. 4. A block diagram of the tomographic algorithm.

[Title Page](#)

[Abstract](#) [Introduction](#)

[Conclusions](#) [References](#)

[Tables](#) [Figures](#)

[⏪](#) [⏩](#)

[◀](#) [▶](#)

[Back](#) [Close](#)

[Full Screen / Esc](#)

[Printer-friendly Version](#)

[Interactive Discussion](#)



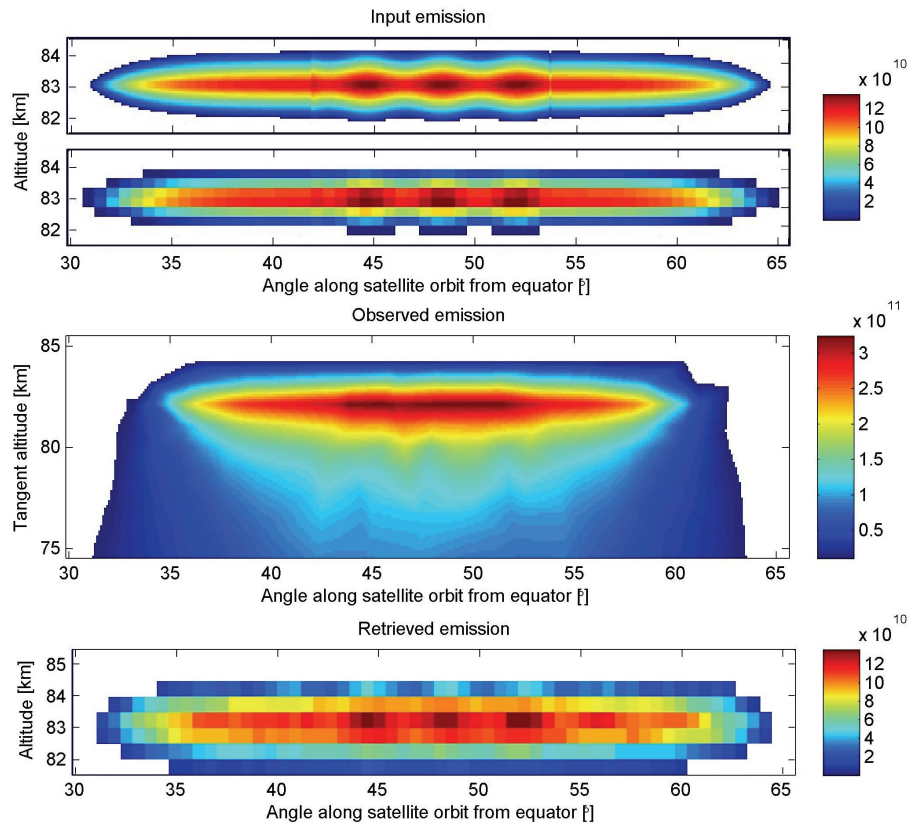


Fig. 5. The steps through a simulated OSIRIS tomography retrieval; the top panel shows an arbitrarily created emission profile, a “test PMC”, and the second panel shows the same profile but with a resolution corresponding to the retrieval grid. The third panel shows simulated OSIRIS observations using the test PMC as input (with both axes referring to the position of the tangent point) and the bottom panel shows the retrieved structure after running the measurements through the tomography algorithm.

Tomographic algorithms for Polar Mesospheric Cloud observations

K. Hultgren et al.

Title Page

Abstract Introduction

Conclusions References

Tables Figures

⏪ ⏩

⏴ ⏵

Back Close

Full Screen / Esc

Printer-friendly Version

Interactive Discussion

Tomographic algorithms for Polar Mesospheric Cloud observations

K. Hultgren et al.

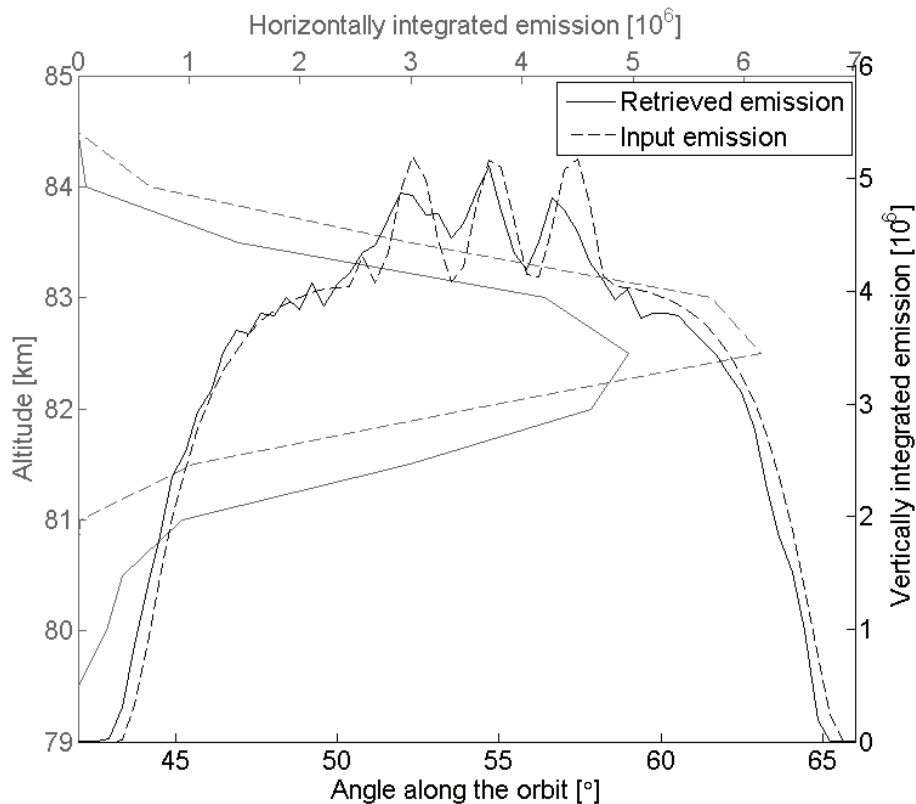


Fig. 6. Integrated vertical and horizontal cross sections of simulated OSIRIS observations. The dashed lines shows emissions from the second panel of Fig. 5 and the solid lines the retrieved result from the bottom panel.

Tomographic algorithms for Polar Mesospheric Cloud observations

K. Hultgren et al.

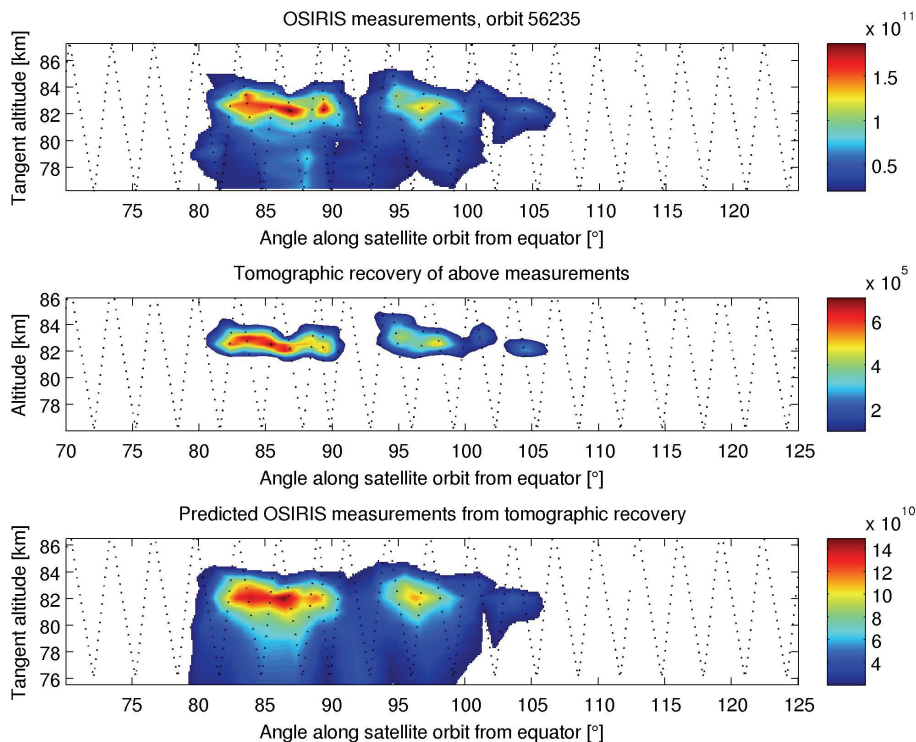


Fig. 7. An example of the tomographic retrieval using real OSIRIS data. The top panel shows the OSIRIS observations plotted as tangent altitude vs. angle along the orbit. The middle panel shows the resulting structure from running the retrieval on the top data. The bottom panel shows predictions of OSIRIS measurements using recovered emissions, for consistency.

[Title Page](#)[Abstract](#)[Introduction](#)[Conclusions](#)[References](#)[Tables](#)[Figures](#)[◀](#)[▶](#)[◀](#)[▶](#)[Back](#)[Close](#)[Full Screen / Esc](#)[Printer-friendly Version](#)[Interactive Discussion](#)